Supporting Information

Materials

All solvents were HPLC and were obtained from Sigma Aldrich or EMD. Commercial chemicals were of reagent grade or better and used without further purification.

^{1}H NMR, ^{13}C NMR and 2D-NMR spectra were recorded on a Varian 400 MHz NMR-System and referenced to the residual proton and carbon signals of the deuterated solvent, respectively.

Low resolution LC/MS (ESI) mass spectra were measured with an Agilent 6130 Quadrupole LC/MS coupled to an Agilent 1200 series HPLC system. High resolution mass spectra were recorded by Q-TOF MS in positive mode and fragmentation by Q-TOF MS-MS by the mass spectrometry laboratory of the University of Illinois.

Preparative scale separation by HPLC was performed using an Agilent 1200 Series HPLC system equipped with a diode array detector (DAD) and a preparative fraction collector using binary solvent gradients as detailed below.

Bacterial strains

Vibrio alginolyticus B522 and *Shewanella algae* B516 were both isolated from a sample of the red seaweed *Chondrus crispus* collected on the shore of Boston, Massachusetts. Bacteria were cultured from cryostocks in nutrient broth E (NBE, 1 g/L meat extract, 2 g/L yeast extract, 5 g/L peptone, 5 g/L NaCl, pH 7.4) at 30°C and 250 rpm.

Sequencing of isolates

16S rDNA sequences were amplified with the commercial standard primer set 8f and 1492r (IDT, ReadyMade Primer) by PCR. Sequencing by Genewiz Inc. was validated by replicates. 16S rDNA data indicated for strain B516 highest homology to *Shewanella algae* and for strain B522 equal homologies with *Vibrio parahaemolyticus* and *Vibrio alginolyticus*. The phylogenetic position of the isolates was further resolved by homologies of maker genes after genome sequencing.

Genome Sequencing

From 1.5 mL of an overnight culture of *V. alginolyticus* B522 in NBE broth genomic DNA was prepared with a GenElute™ Bacterial Genomic DNA kit (Sigma Aldrich). The genome was sequenced by Next-Generation Sequencing with 100 bp single end reads using Illumina of the Harvard Biopolymers Facility.

Phylogenetic analyses

Any phylogenetic analyses reported here was performed using sequence alignment in ClustalW2 and construction of maximum likelihood trees using TREEFINDER (G. Jobb, TREEFINDER version of March 2011, Munich, Germany [www.treefinder.de]) from 1000 replicates with LR-ELW edge support as bootstrap.

Identification of the *Shewanella* strain on species level was performed using *gyrB* gene sequences that have been used before to obtain phylogenetic species resolution.[22] Strain B516 hereby clustered with *S. algae* confirming the assignment by 16S rDNA (Figure S1).

The amino acid sequences of the individual putative gene products of the avaroferrin gene cluster were aligned with their homologs of the biosynthetic gene clusters of bisucaberin of *Aliivibrio salmonicida* LFI1238 (BibA-C), putrebactin of *Shewanella putrefaciens* 200 (PubA-C), alcaligin of *Bordetella bronchiseptica* RB50 (AlcA-C), desferrioxamine of *Streptomyces coelicolor* A3(2) (DesA-D), and the gene products of an uncultured bacterium (MbsA-D) and the reconstructed maximum likelihood trees are given in figure S14.

Swarming assay

Standard swarming assays were performed on κ-carrageenan NBE plates, prepared from 1.5 % (w/v) carrageenan for gel preparation (Sigma Aldrich, CAS: 9000-07-1) in Nutrient Broth E (NBE, 1 g/L meat extract, 2 g/L yeast extract, 5 g/L peptone, 5 g/L NaCl, pH 7.4) with 25 mL per 100 mm plate. A 6 mm blank paper disc (BBL, Becton, Dickson and Company) was placed in the center of a plate surrounded by four further blank paper discs with 2 cm distance between the centres of each disc. The central disc was inoculated with 5 µL overnight culture of *V. alginolyticus* B522 in NBE medium and incubated at 30°C. After 14 h the surrounding discs were inoculated with 5 µL of a DMSO stock of the test compound. Assays were generally carried out at least as independent triplicates on different plates.

Image Analysis

Time-lapse microscopic image series (31 frames, total of 15sec) were analysed in MATLAB using our analysis tools that we developed and described recently.[23] We applied whole image series temporal variance analysis from high resolution DIC microscopic time-lapse series of swarming cells to obtain an integrated measure of relative motion. For histograms, three to five spots in a distinct zone were analysed and averaged for each experiment and at least three different experiments were evaluated. Additional data are shown in Figure S2. Moving window temporal variance analysis gave the fraction of time with significant temporal variance which corresponds to the fraction of time spent moving. This analysis method produced heat maps that demonstrate that cells spend more time stationary than moving within in the macroscopic zone of inhibition (Figure S3).

Standard LC-MS method for siderophores

Avaroferrin, putrebactin and bisucaberin were analyzed by low resolution LC/MS (ESI) by injecting 20 µL on a Phenomenex Luna 5u C18 (100Å, 5 micron, 100 x 4.60 mm) using a gradient of water/acetonitrile + 0.1% formic acid at a flow rate of 0.5 mL/min (A = water + 0.1% formic acid, B = acetonitrile + 0.1% formic acid, gradient: T_0: B = 5%; $T_{18\ min}$: B = 75%; $T_{20\ min}$: B = 75%, T_{21}: B = 5%; $T_{23\ min}$: B = 5%).

Purification of avaroferrin

For extraction of the natural product, 100 µL of an overnight culture of *Shewanella algae* strain B516 in NBE medium were plated on 18 large (150 x 15 mm) κ-carrageenan NBE plates, each. The plates were incubated for 2 days at 30°C, then chopped in pieces and soaked over night in 1.5 L ethyl acetate. The ethyl acetate extract was discarded and the residual material was soaked for two days in 1.5 L isopropanol. The isopropanol was filtered and evaporated. The residue was taken up in little methanol diluted with deionised water to less than 5% methanol. The solution was loaded on a Sep-Pak Vac 35cc (10g) C18 cartridge (Waters) and eluted subsequently with water, 30% methanol and 60% methanol in water. The active fraction (containing avaroferrin) eluted at 30% methanol. This fraction was pooled, evaporated and the residue was subjected to preparative HPLC on a Phenomenex Luna 5u C18(2) AXIA Pac column (100Å, 5 micron, 250 x 21.20 mm) using a gradient of water/methanol at a flow rate of 10 mL/min (A = water, B = methanol, gradient: T_0: B = 10%; $T_{25\ min}$: B = 60%; $T_{30\ min}$: B = 100%). Fractions of four individual HPLC runs were collected in fraction sizes of 10 mL, each. The activity was found in the fractions with 22-23 min retention time. These fractions were pooled and purified by preparative HPLC on a Phenomenex Luna 10u Phenyl Hexyl column (100Å, 10 micron, 250 x 21.20 mm) using a gradient of water/methanol at a flow rate of 10 mL/min (A = water, B = methanol, gradient: T_0: B = 10%; $T_{5\ min}$: B = 25%; $T_{30\ min}$: B = 50%, $T_{35\ min}$: B = 100%). The active fraction eluted at 26 min retention time as a single peak in the UV-spectrum at 220 nm, resulting in 1.18 mg pure avaroferrin.

The compound was identified by ^{1}H and ^{13}C NMR in DMSO-d_6 and CD_3OD in combination with 2D homo- and heteronuclear experiments comprising COSY, HSQC, HMBC, and ROESY spectra (Figures S5-11). High resolution Q-TOF mass spectrometry in positive mode (m/z): 387.2248 $[M+H]^+$ (calc. 387.2244). Low resolution Q-TOF mass spectrometry in positive mode (m/z): 387.2 $[M+H]^+$ (100% relative intensity), 409.2 $[M+Na]^+$ (20% relative intensity). MS-MS resulted in two different fragmentation products (Figure S12).

X-ray crystallography

Purified avaroferrin was crystallized from methanol by slow evaporation in a 3 mm NMR tube. The structure was determined by X-ray diffraction at the Harvard University Center for Crystallographic Studies. Data were collected at 100 K from a crystal mounted on a Bruker APEX II DUO CCD

diffractometer ($Cu_{K\alpha}$ radiation, λ = 1.54178 Å) equipped with an Oxford Cryosystems nitrogen flow apparatus. The collection method involved 1.0° scans in ω at 30°, 55°, 80° and 115° in 2θ. Data integration down to 0.84 Å resolution was carried out using SAINT V7.46 A (Bruker diffractometer, 2009) with reflection spot size optimization. Absorption corrections were made with the program SADABS (Bruker diffractometer, 2009). The structure was solved by the direct methods procedure and refined by least-squares methods again F^2 using SHELXS-97 and SHELXL-97.[24] Non-hydrogen atoms were refined anisotropically, and hydrogen atoms were allowed to ride on the respective atoms. Crystal data as well as details of data collection and refinement are summarized in Table S1 and Figure 1C.

Purification of putrebactin and bisucaberin

For extraction of the natural products, 40 µL of an overnight culture of *Shewanella algae* strain B516 in NBE medium were plated on 14 large (150 x 15 mm) κ-carrageenan NBE plates, each. The plates were incubated for 4 days at 30°C, then chopped in pieces and soaked for three days in 1.5 L isopropanol. The isopropanol was filtered and evaporated. The residue was taken up in little methanol diluted with deionised water to less than 5% methanol. The solution was loaded on a Sep-Pak Vac 35cc (10g) C18 cartridge (Waters) and eluted subsequently with water, 30% methanol and 60% methanol in water and collected in approximately 15 mL fractions. Target compounds were detected by mass spectrometry as described above (Standard LC-MS method for siderophores) and purified according to the mass traces of putrebactin and bisucaberin. Putrebactin eluted early at 30% methanol while bisucaberin eluted later at 30% methanol and could be separated already in the first step. Fractions with avaroferrin were overlapped the putrebactin and bisucaberin fractions. This fractions that were identified to contain putrebactin were pooled, evaporated and the residue was subjected to preparative HPLC on a Phenomenex Luna 5u C18(2) AXIA Pac column (100Å, 5 micron, 250 x 21.20 mm) using a gradient of water/methanol at a flow rate of 10 mL/min (A = water, B = methanol, gradient: T_0: B = 35%; $T_{25\ min}$: B = 60%; $T_{28\ min}$: B = 100%). Fractions of four individual HPLC runs were collected in fraction sizes of 10 mL, each. The mass of putrebactin was found in the fractions with 10-13 min retention time together with avaroferrin. These fractions were pooled and purified by preparative HPLC on a Phenomenex Luna 5u C18(2) AXIA Pac column (100Å, 5 micron, 250 x 21.20 mm) using a gradient of water/acetonitrile + 0.1% formic acid at a flow rate of 10 mL/min (A = water + 0.1% formic acid, B = acetonitrile + 0.1% formic acid, gradient: T_0: B = 10%; $T_{5\ min}$: B = 10%; $T_{30\ min}$: B = 25%) in three individual runs. The mass of putrebactin was found in the fraction with 19 min retention time, while avaroferrin eluted at 22-23 min retention time. The putrebactin containing fraction was further purified on a Phenomenex Luna 10u Phenyl Hexyl column (100Å, 10 micron, 250 x 21.20 mm) using a gradient of water/acetonitrile + 0.1% formic acid at a flow rate of 10 mL/min (A = water + 0.1% formic acid, B = acetonitrile + 0.1% formic acid, gradient: T_0: B = 10%; $T_{5\ min}$: B = 10%; $T_{30\ min}$: B = 35%) where the mass of putrebactin was found in the fractions with 18-19 min

retention time. This was followed by a final purification step on a Phenomenex Luna 5u C18(2) AXIA Pac column (100Å, 5 micron, 250 x 21.20 mm) using a gradient of water/acetonitrile + 0.1% formic acid at a flow rate of 10 mL/min (A = water + 0.1% formic acid, B = acetonitrile + 0.1% formic acid, gradient: T_0: B = 10%; $T_{5\ min}$: B = 14%; $T_{35\ min}$: B = 22%). The pure compound was obtained at 15 min retention time and was confirmed by NMR as putrebactin with a total yield of 0.70 mg.

The compound was identified by ^{1}H and ^{13}C NMR in DMSO-d_6 in combination with 2D homo- and heteronuclear experiments comprising COSY, HSQC, HMBC, and ROESY spectra as putrebactin as known in the literature (Figure S16).[8] High resolution Q-TOF mass spectrometry in positive mode (m/z): 373.2095 $[M+H]^+$ (calc. 373.2087).

The bisucaberin containing fractions of the initial elution from the Sep-Pak C18 cartridge were pooled, evaporated and the residue was subjected to preparative HPLC on a Phenomenex Luna 5u C18(2) AXIA Pac column (100Å, 5 micron, 250 x 21.20 mm) using a gradient of water/methanol at a flow rate of 10 mL/min (A = water, B = methanol, gradient: T_0: B = 25%; $T_{30\ min}$: B = 60%; $T_{32\ min}$: B = 100%) in three individual runs. The mass of bisucaberin was found in the fractions with 22-27 min retention time together with avaroferrin. These fractions were pooled and purified by preparative HPLC on a Phenomenex Luna 5u C18(2) AXIA Pac column (100Å, 5 micron, 250 x 21.20 mm) using a gradient of water/acetonitrile + 0.1% formic acid at a flow rate of 10 mL/min (A = water + 0.1% formic acid, B = acetonitrile + 0.1% formic acid, gradient: T_0: B = 10%; $T_{5\ min}$: B = 15%; $T_{30\ min}$: B = 30%). The pure compound was obtained at 19 min retention time and was confirmed by NMR as bisucaberin with a total yield of 0.74 mg.

The compound was identified by ^{1}H and ^{13}C NMR in DMSO-d_6 in combination with 2D homo- and heteronuclear experiments comprising COSY, HSQC, HMBC, and ROESY spectra as bisucaberin as known in the literature (Figure S15).[9] High resolution Q-TOF mass spectrometry in positive mode (m/z): 401.2394 $[M+H]^+$ (calc. 401.2400).

Comparison of siderophore production

Shewanella algae strain B516 overnight cultures in NBE medium were plated on 6 large (150 x 15 mm) κ-carrageenan NBE plates with 40 µL, each. The plates were incubated for three days at 30°C, then chopped in pieces and the material of two plates with three replicates was soaked for three days in 200 mL isopropanol. The isopropanol was filtered off and the residual plate material was washed with 50 mL isopropanol. The isopropanol fractions were pooled, evaporated and taken up in 400 mL methanol. Of each sample 20 µL were subjected to LC-MS analysis on a Phenomenex Luna 5u C18 column (100Å, 5 micron, 100 x 4.6 mm) using a gradient of water/acetonitrile with 0.1% formic acid at a flow rate of 0.5 mL/min (A = water + 0.1% formic acid), B = acetonitrile + 0.1% formic acid), gradient: T_0: B = 5%; $T_{18\ min}$: B = 75%; $T_{20\ min}$: B = 75%; $T_{21\ min}$: B = 5%; $T_{23\ min}$: B = 5%).

The masses of the protonated siderophores were extracted from the total ion count and the peak areas integrated. The relative abundance were 1.98 ± 0.11 for avaroferrin, 1.08 ± 0.06 for putrebactin, and 1.02 ± 0.03 for bisucaberin.

Microscope data acquisition

Swarming plate assays were set up as described above with *V. alginolyticus* B522 in the center and *S. algae* B516 (5 µL overnight culture), the purified avaroferrin (5 µL of 10 mM DMSO stock), and DMSO as control. The plates were incubated until the swarming inhibition zone became clearly visible. A square of approximately 8 mm was cut out from carrageenan plates with a scalpel including the inhibition zone and an equal part of the area before the inhibition zone. The cut out square was placed top-down on a glass bottom microwell dish (MatTek, 35 mm petri dish, 14 mm microwell, No. 1.5 cover glass). It is important to not move the sample to avoid shear forces which reduce the overall motility of the cells in the sample. Microwell dishes were mounted on a Prior ProScan II motorized stage and imaged at room temperature. All images were collected with a Nikon Ti motorized inverted microscope equipped with a Plan Apo 100x 1.4 NA objective lens and DIC optics. Images were acquired with a Hamamatsu ORCA-R2 cooled-CCD camera controlled with MetaMorph 7 software. For time-lapse experiments, images were collected every 500ms using a 40ms exposure time, for a duration of 15sec. Measurements were taken inside and outside of the inhibition zone for each sample with at least five measurement points, each. Experiments were carried out in triplicates from three independent plates, each.

Determination of pM(Fe^{III})

The pM(Fe^{III}) values of avaroferrin, bisucaberin, and putrebactin were determined as described by Abergel et al. by competition with EDTA.[15] The experiments were carried out at pH 7.4 in HEPES buffer (10 mM HEPES (2-[4-(2-hydroxyethyl)piperazin-1-yl]ethanesulfonic acid), 0.2 M KCl, pH 7.4) with 0.1 mM $FeCl_3$ and 0.1 mM of the respective siderophore. Experiments were carried out with variable EDTA concentrations ranging from 0.01 mM to 5 mM in 100 µL volumes. The reactions were allowed to equilibrate for at least 24 h and UV-absorption spectra were recorded with a Ultrospec 5300 *pro* UV/Vis-spectrophotometer (Amersham Biosiences) in UV-micro cuvettes (Brand). The absorption at 430 nm was used to quantify the amount of Fe-siderophore complex in relation to Fe-EDTA and data were processed using the equations derived by Abergel et al to obtain ΔpM values that allowed to derive pM(Fe^{III}) values from the known stability constant of EDTA (pM(Fe^{III}) = 23.4).[15] Multiple data titrations gave pM(Fe^{III}) values with standard deviation as shown in Figure S18.

Iron chelators

Various iron chelators were used to test the effect of swarming inhibition under iron limitation. The chelators and siderophores were used as stocks in DMSO. The compounds purchased were:

deferoxamine (mesylate salt, Sigma-Aldrich), ferrichrome (iron-free from Ustilago sphaerogena, Sigma-Aldrich), quercetin (Sigma-Aldrich), 2,3-dihydroxybenzoic acid (Sigma-Aldrich), deferasirox (Selleck Chemicals).

Growth assay

Avaroferrin was reconstituted in NBE medium inoculated with 1:1000 *V. alginolyticus* B522 to obtain concentrations of 100 µM, 500 µM, and 1000 µM. The bacteria were grown with an untreated control in triplicates of 50 µL in a 96 well plate at 30°C shaking at 250 rpm. Growth was determined by measuring the absorption at 600 nm at different time points.

Table S1. Crystal data and data on collection and refinement for avaroferrin.

Crystal data	
Crystal system, space group	Monoclinic, *Pc*
a, *b*, *c* (Å)	9.0012 (2), 11.5094 (2), 9.4906 (2)
β (°)	101.447 (1)
V (Å^3)	963.65 (3)
Z	2
Radiation type	Cu *K*α
μ (mm^{-1})	0.84
Crystal size (mm)	0.18 × 0.16 × 0.10
Data collection	
Absorption correction	Multi-scan *SADABS*
T_{min}, T_{max}	0.863, 0.920
No. of measured, independent and observed [$I > 2\sigma(I)$] reflections	19966, 3183, 3096
R_{int}	0.030
$(\sin \theta/\lambda)_{max}$ (Å^{-1})	0.594
Refinement	
$R[F^2 > 2\sigma(F^2)]$, $wR(F^2)$, S	0.034, 0.092, 1.06
No. of reflections	3183
No. of parameters	274
No. of restraints	56
H-atom treatment	H-atom parameters constrained
$\Delta\rho_{max}$, $\Delta\rho_{min}$ (e Å^{-3})	0.13, -0.21

Table S2: Proteins of the avaroferrin gene cluster with proposed functions according to protein sequence homologies with the corresponding percentage of identities.

Proteine	**Proposed function**	**Homology**
AvbA	Decarboxylase (cadaverine biosynthesis)	BibA, *Aliivibrio* (57%)
AvbB	Monooxygenase (hydroxamate biosynthesis)	PubA, *Shewanella* (63%)
AvbC	Siderophore biosynthesis protein I	$BibC^{N}$, *Aliivibrio/Shewanella* (45%)
AvbD	Siderophore biosynthesis protein II	PubC, *Shewanella* (64%)
AvtA	TonB-dependent siderophore receptor	PutA, *Shewanella* (65%)
AvtB	iron-siderophore ABC transporter periplasmic binding protein	BitB, *Aliivibrio* (57%)
AvtC	iron-siderophore ABC transporter membrane permease component	BitC, *Aliivibrio* (58%)
AvtD	iron-siderophore ABC transporter membrane permease component	BitD, *Aliivibrio* (60%)
AvtE	iron-siderophore ABC transporter ATP-binding protein	BitE, *Aliivibrio* (61%)
AvtF	ferric iron reductase	PutB, *Shewanella* (30%)
AvtG	TonB-dependent receptor	*Shewanella* (73%)
AvtH	periplasmic siderophore cleavage esterase IroE family	*Shewanella* (41%)

Table S3: Chelators.

Compounds	MSID	pFe(III)	Ref.
2,3-Dihydroxybenzoic acid	>500 nmol	NA	
Quercetin	250 nmol	NA	
Deferasirox	5 nmol	22.5	[25]
Deferoxamine B	>500 nmol	26.6	[26]
Ferrichrome	>500 nmol	25.2	[26]

MSID: minimum swarming inhibiting dose, NA: not available

Table S4: Putative siderophore uptake, iron acquisition and storage related proteins found by homology in the genome of *V. alginolyticus* B522.

Sequence ID	Predicted function	Homology Sequence ID
Siderophore-Iron uptake		
B522_528	TonB-dependent hemoglobin/transferrin/lactoferrin receptor	WP_009704939
B522_732	TonB-dependent siderophore receptor/Ferric vibrioferrin receptor	WP_005395582
B522_733	TonB-dependent siderophore receptor	YP_003288217
B522_1051	TonB-dependent siderophore receptor/Enterobactin receptor	WP_005450185
B522_1295	Ferric siderophore transporter binding protein TonB	YP_003287995
B522_1300	putative ferrichrome-iron receptor	WP_005393534
B522_1680	ferric aerobactin receptor precursor	WP_005376064
B522_1744	TonB-dependent hemoglobin/transferrin/lactoferrin receptor	WP_009704439
B522_2063	ferric siderophore transporter binding protein TonB	YP_003288503
B522_2493	ferrichrome-iron receptor	YP_003286192
B522_2851	TonB-denpendent receptor	WP_005379366
B522_2856	ferric siderophore transport system binding protein TonB	YP_003284488
B522_3116	enterobactin receptor	WP_005397184
B522_3304	ferrichrome-iron receptor	YP_003285946
B522_3550	TonB-dependent heme receptor	WP_005391429
B522_4069	TonB-dependent receptor domain protein	WP_005393952
B522_4703	Ferrichrome-iron receptor	YP_007301337
B522_869	utilization protein for catechol-siderophore/vulnibactin	WP_005497727
B522_2068	hemin import ATP-binding protein	WP_005385036
B522_2765	iron transporter FeoB	WP_005388355
Iron storage		
B522_4284	bacterioferritin	WP_005381359
B522_2943	ferritin	YP_003284573
B522_2047	Iron-binding ferritin-like antioxidant protein	WP_002541766
B522_2798	ferrochelatase	WP_005384976
Vibrioferrin biosynthesis		
B522_734	vibrioferrin biosynthesis protein PvsA	BAC16544
B522_735	vibrioferrin biosynthesis protein PvsB	YP_007301552
B522_736	vibrioferrin membrane-spanning transport protein PvsC	YP_007301553
B522_737	vibrioferrin biosynthesis protein PvsD	BAC16547
B522_738	vibrioferrin biosynthesis protein PvsE	BAC16548
Membrane Transporter		
B522_730	ferrichrome ABC transporter (permease) PvuC	YP_007301547
B522_3110	enterochelin ABC transporter substrate-binding protein	WP_005376635
B522_3111	enterochelin ABC transporter permease	WP_009704146
B522_3112	iron(III) ABC transporter permease	WP_005397178
B522_3113	iron(III) ABC transporter ATP-binding protein	WP_005376629
B522_3720	iron(III) ABC transporter substrate-binding protein	WP_005386566
B522_728	iron ABC transporter	WP_005374717

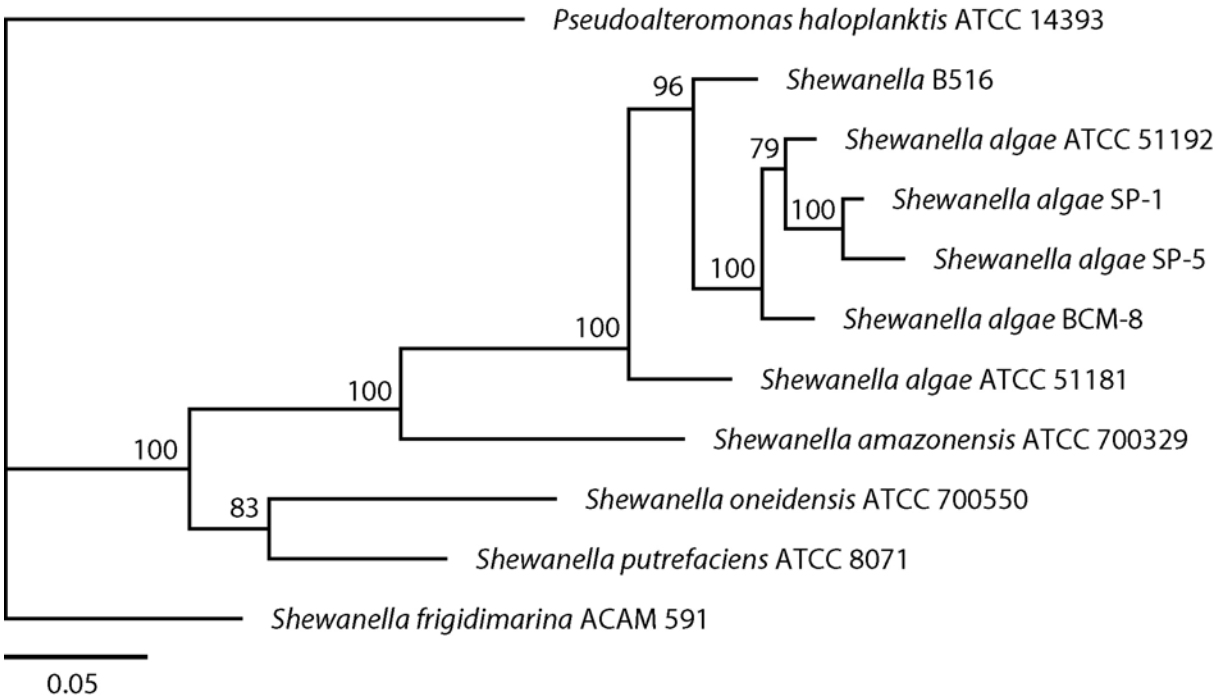

Figure S1: Maximum likelihood phylogenetic analysis of *gyrB* gene sequences. *Pseudoalteromonas haloplanktis* was used as outgroup. Bootstrap values of 1000 re-samplings are given at branching points. The scale bar indicates 5% nucleotide substitutions per site.

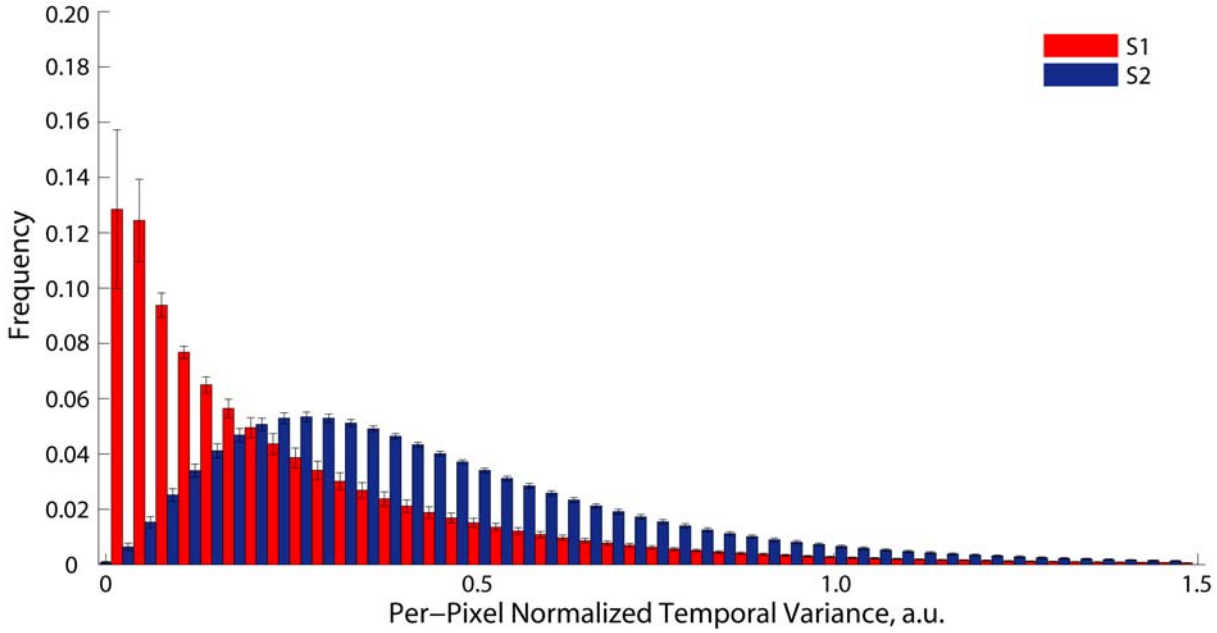

Figure S2: An additional sample set showing the difference between motion activity as per-pixel normalized temporal variance of time-lapse image series within the zone of inhibition close to *S. algae* B516 (S1) and outside the zone close to the colony of *V. alginolyticus* B522 (S2).

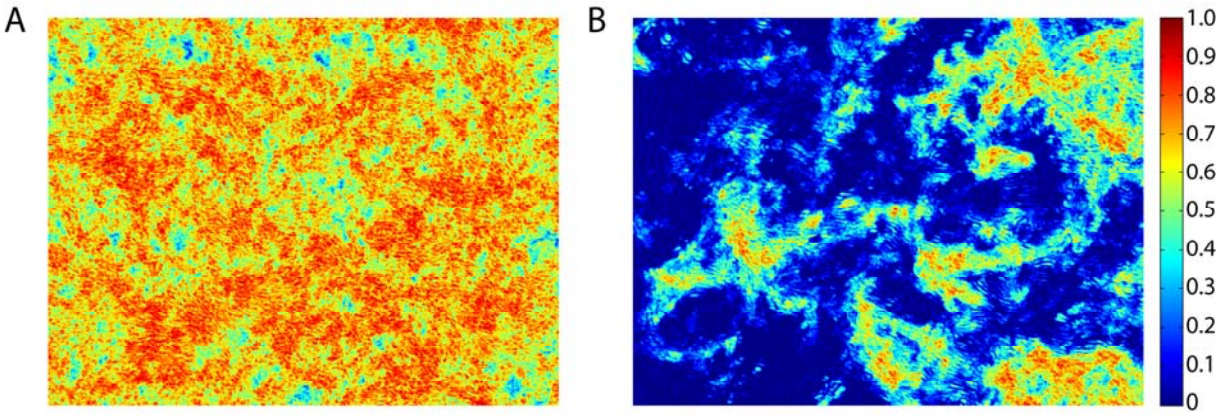

Figure S3: Heat maps showing the fraction of time with significant temporal variance corresponding to the relative fraction of time of swarming cells spent moving (color coding: red = large fraction of time with significant variance, blue = small fraction of time with significant variance). A) Zone close to the colony of *V. alginolyticus* (S1) and B) inhibition zone (S2). Cells in the inhibition zone spend more time stationary than moving while cells in zone S1 are continuously moving.

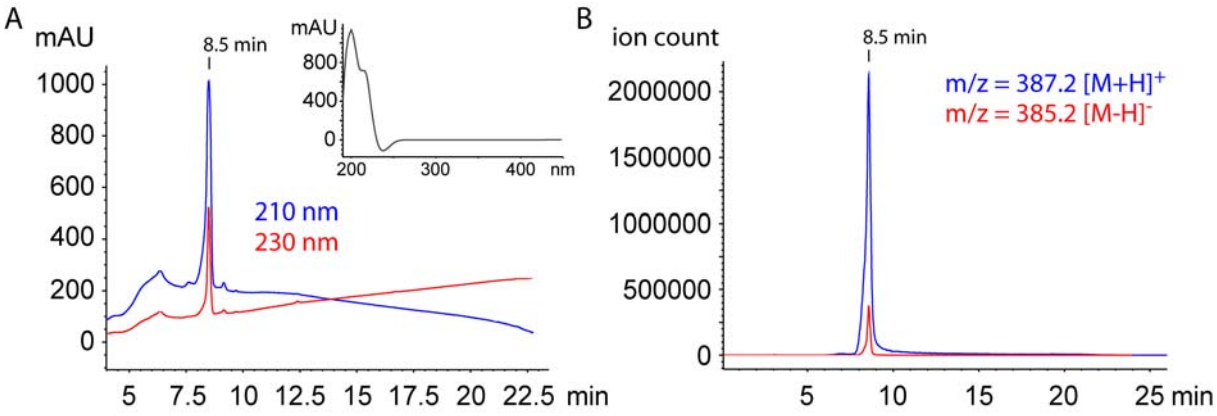

Figure S4: Isolation of avaroferrin. A) Analytical HPLC spectrum at 210 and 230 nm. Inset: UV absorption spectrum of the compound at 8.5 min retention time. B) Extracted ions in positive and negative mode ESI-MS correlate with the retention time of the isolated peak in the UV spectrum.

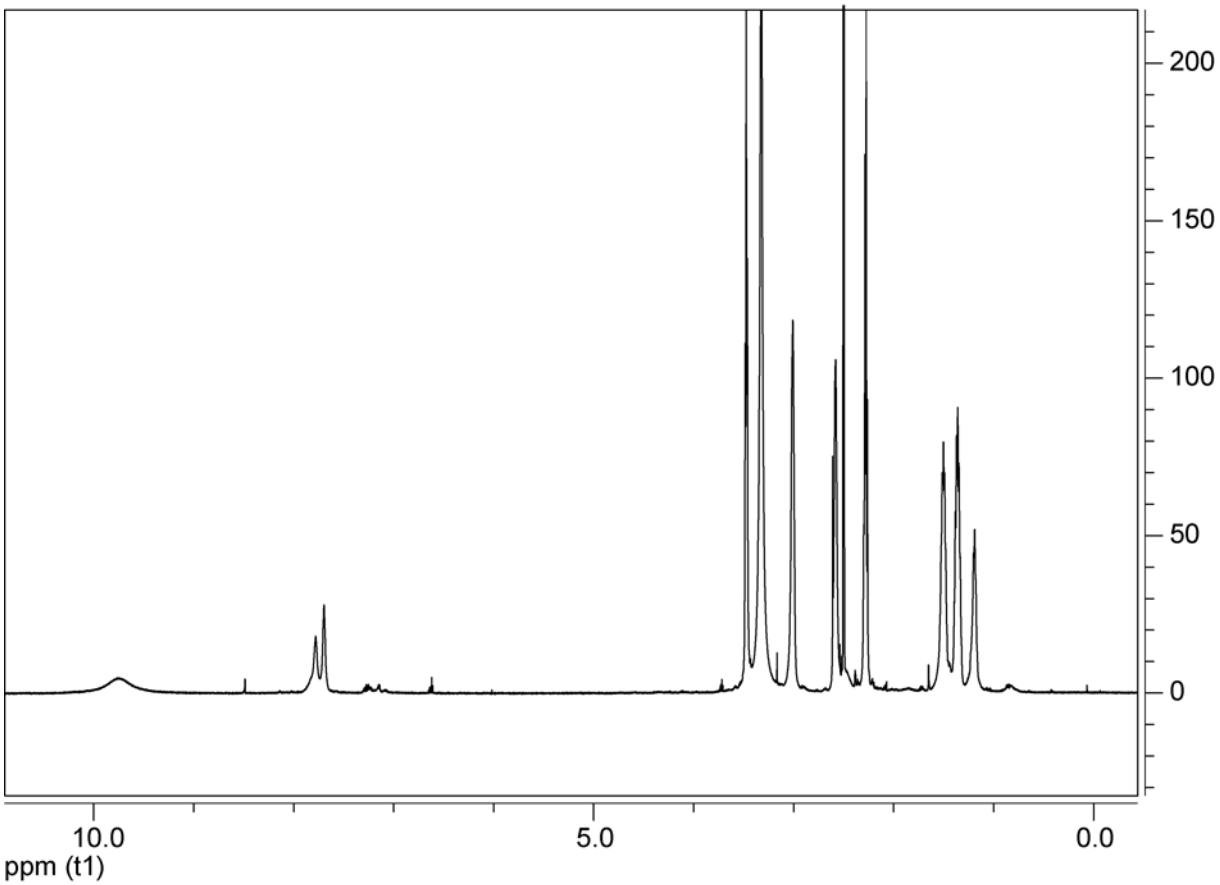

Figure S5: ^{1}H NMR spectrum of avaroferrin at 600 MHz in DMSO-d_6.

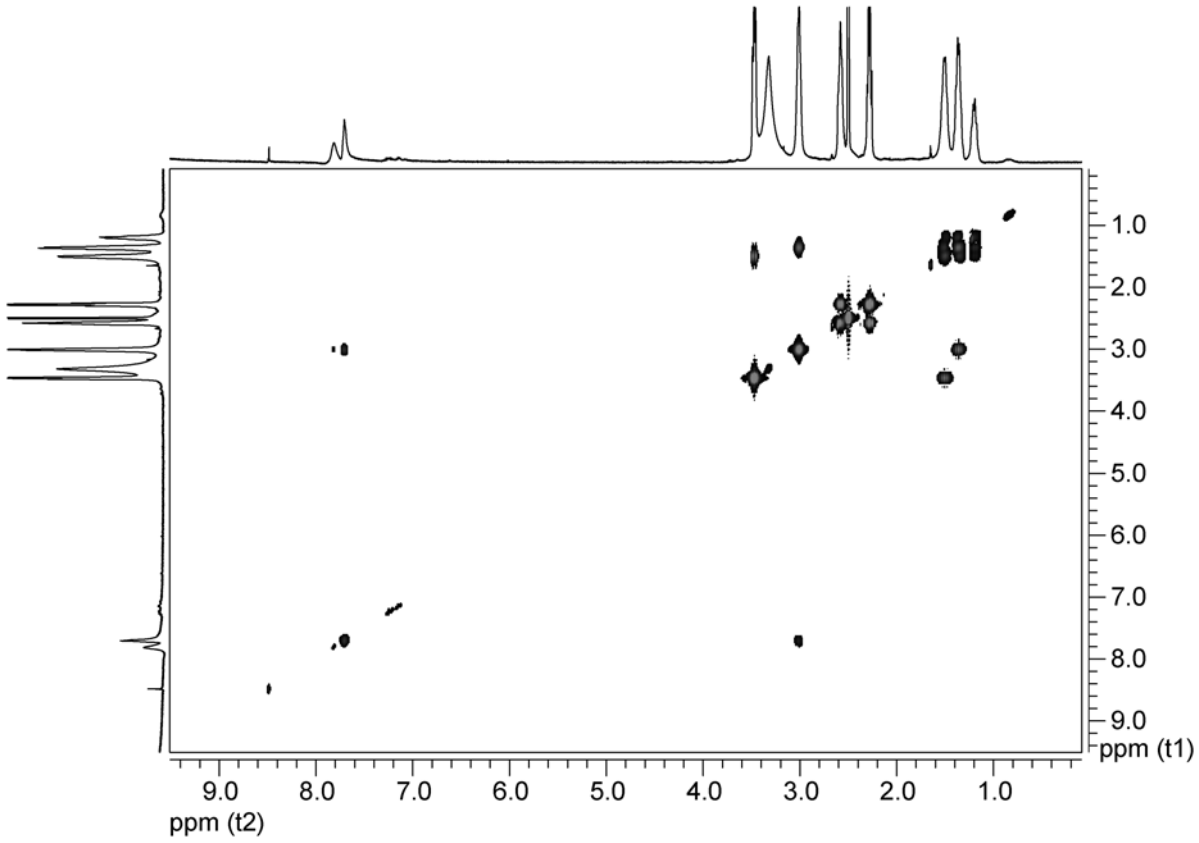

Figure S6: gCOSY spectrum of avaroferrin at 600 MHz in DMSO-d_6.

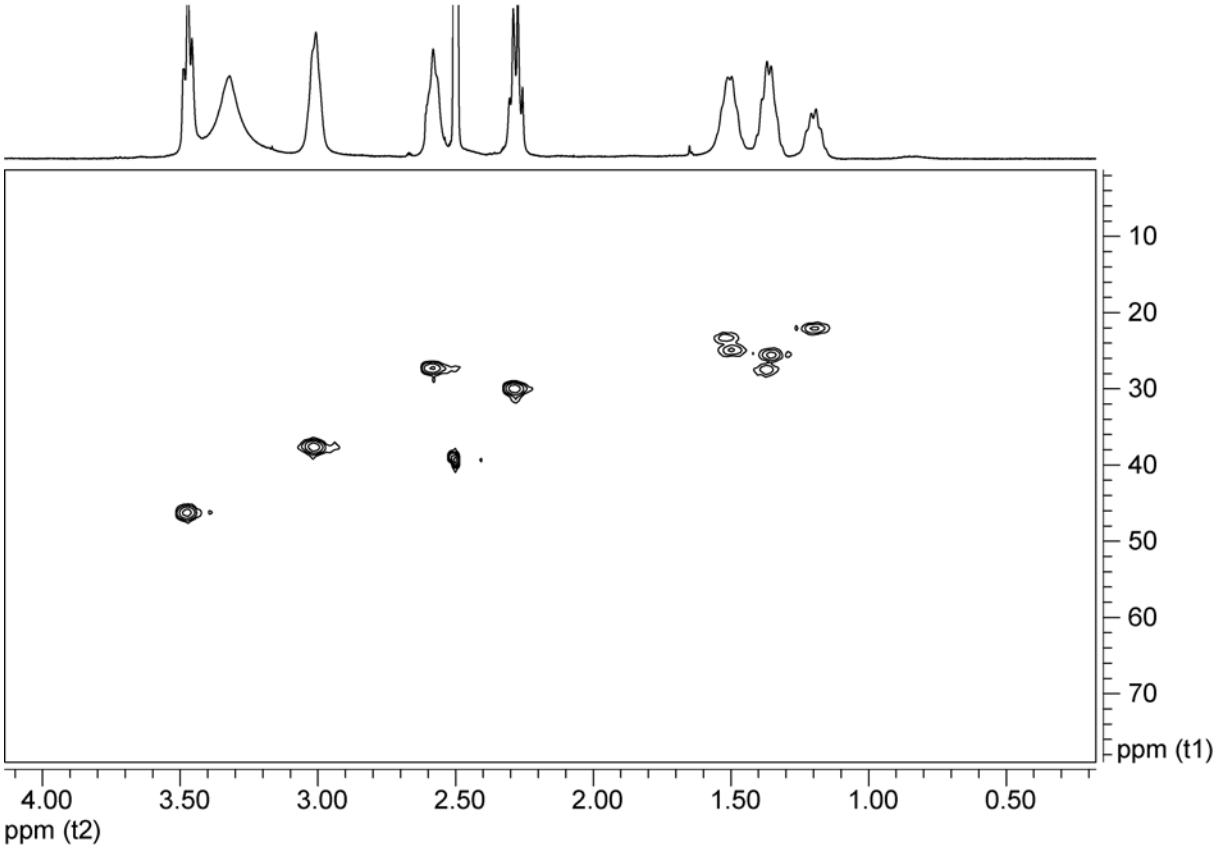

Figure S7: gHSQCAD spectrum of avaroferrin at 600 MHz in DMSO-d_6.

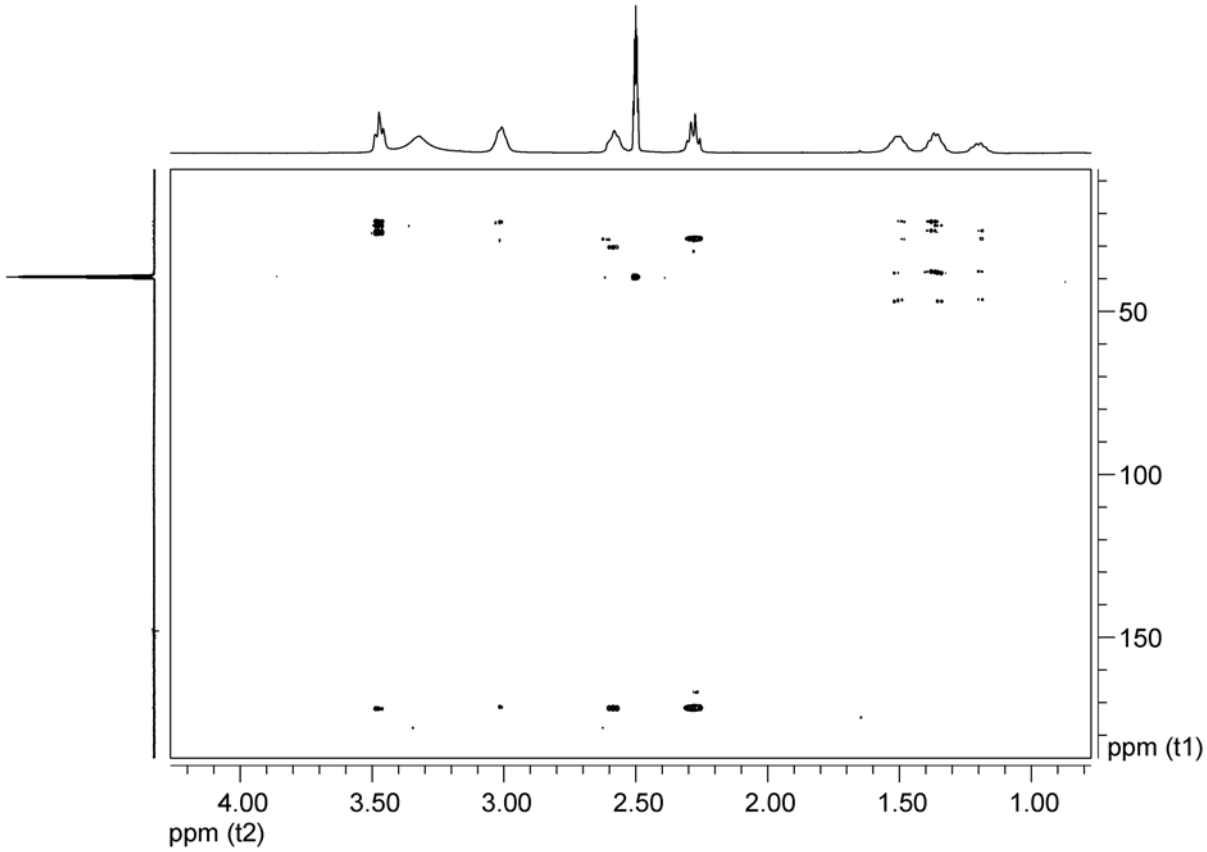

Figure S8: gHMBCAD spectrum of avaroferrin at 600 MHz in DMSO-d_6.

Avaroferrin

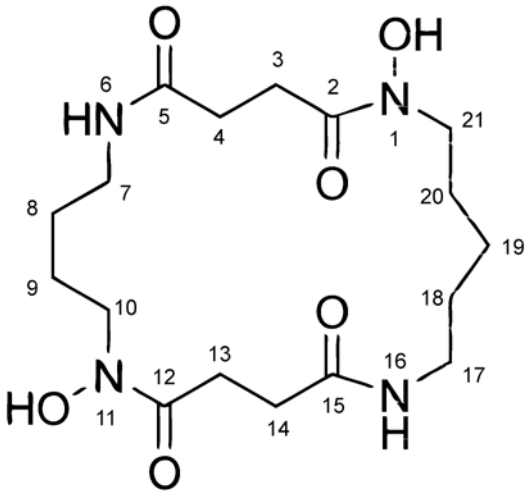

Position	DMSO-d_6		CD_3OD	
	δ ^{1}H (multip., J, no. H)	δ ^{13}C	δ ^{1}H (multip., J, no. H)	δ ^{13}C
1 /11 (N-OH)	9.76 (br s, 2H)			
2/12		171.8		174.6
3/13	2.61 (br, 4H)	27.6	2.77 (m, 4H)	28.9
4/14	2.28 (m, 4H)	30.4	2.47 (m, 4H)	31.9
5/15		171.5		175.1
6/16 (NH)	7.82(br s, 1H), 7.71 (br s, 1H)			
7	3.01 (br, 4H)	38.3	3.18 (m 4H)	40.3
17		37.9		39.9
8	1.35 (m, 2H)	26.0	1.51 (m, 2H)	27.2
9	1.51 (m, 2H)	23.7	1.67 (Ψp, 6.9 Hz, 2H)	25.2
10	3.47 (Ψt, 6.2 Hz, 4H)	46.9	3.63 (t, 6.8 Hz, 2H)	48.9*
21		46.4	3.62 (t, 6.6 Hz, 2H)	48.2*
18	1.38 (m, 2H)	27.7	1.52 (m, 2H)	29.3
19	1.19 (Ψp, 7.0 Hz, 2H)	22.5	1.31 (Ψp, 7.3 Hz, 2H)	24.1
20	1.50 (m, 2H)	25.3	1.62 (Ψp, 6.7 Hz, 2H)	26.8

*^{13}C peaks covered by CD_3OD peak, δ inferred from HMBC data

Figure S9: ^{1}H and ^{13}C NMR data for avaroferrin including chemical shifts, multiplicities, *J*-coupling and number of protons.

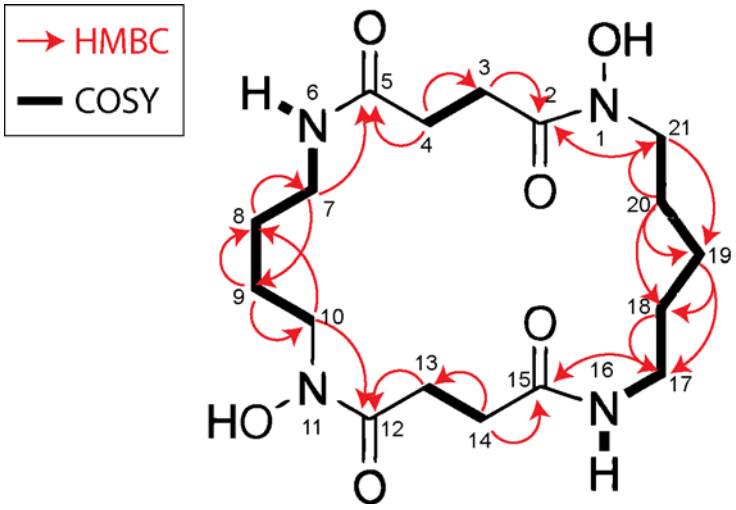

Figure S10: 2D NMR correlations of COSY and HMBC experiments.

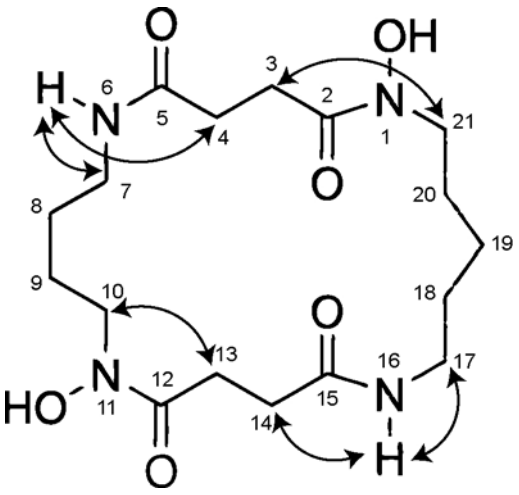

Figure S11: 2D NMR correlations of a ROESY experiment.

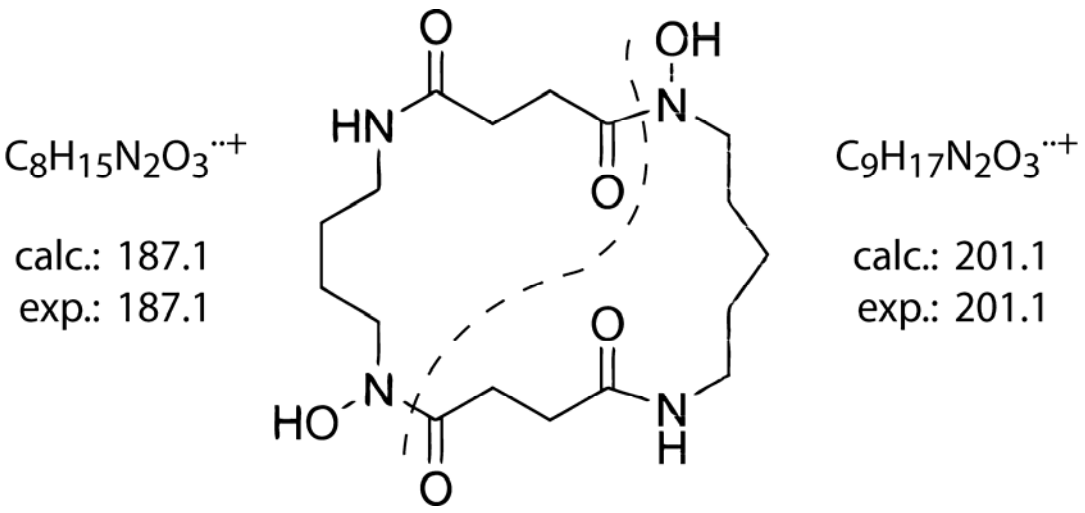

Figure S12: Fragmentation pattern in Q-TOF MS-MS analysis of avaroferrin.

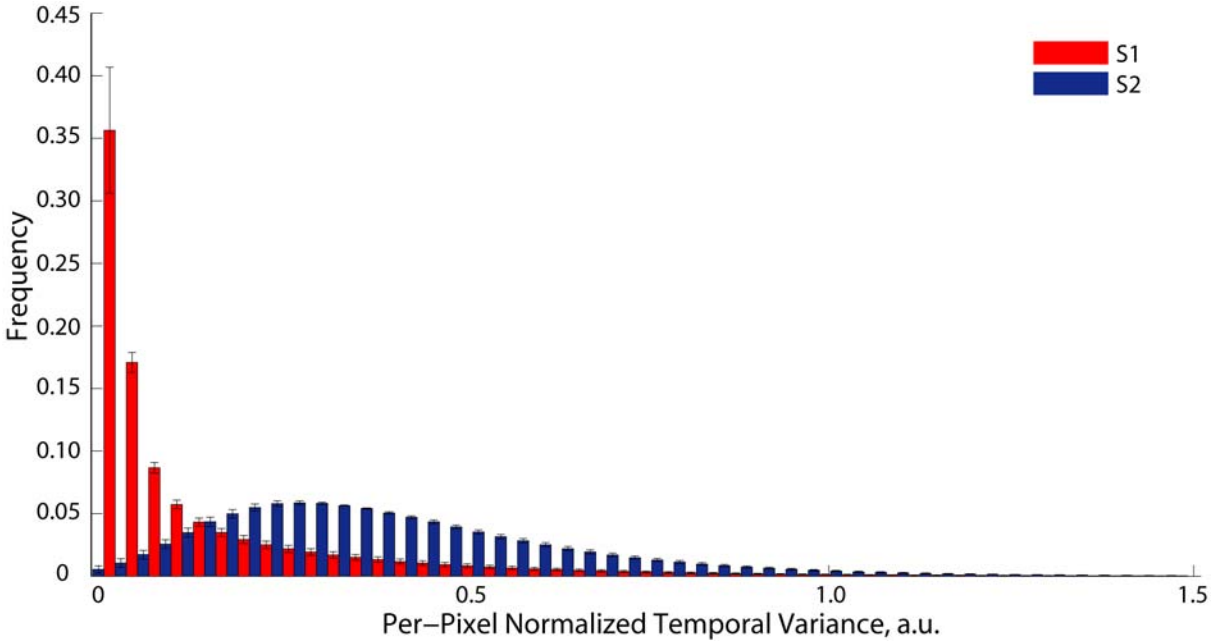

Figure S13: Per-pixel normalized temporal variance of time-lapse image series within the zone of inhibition of avaroferrin applied at 50 nmol on the plate (S1) and outside the zone close to the colony of *V. alginolyticus* B522 (S2) shows dramatically reduced swarming motility as result of avaroferrin treatment.

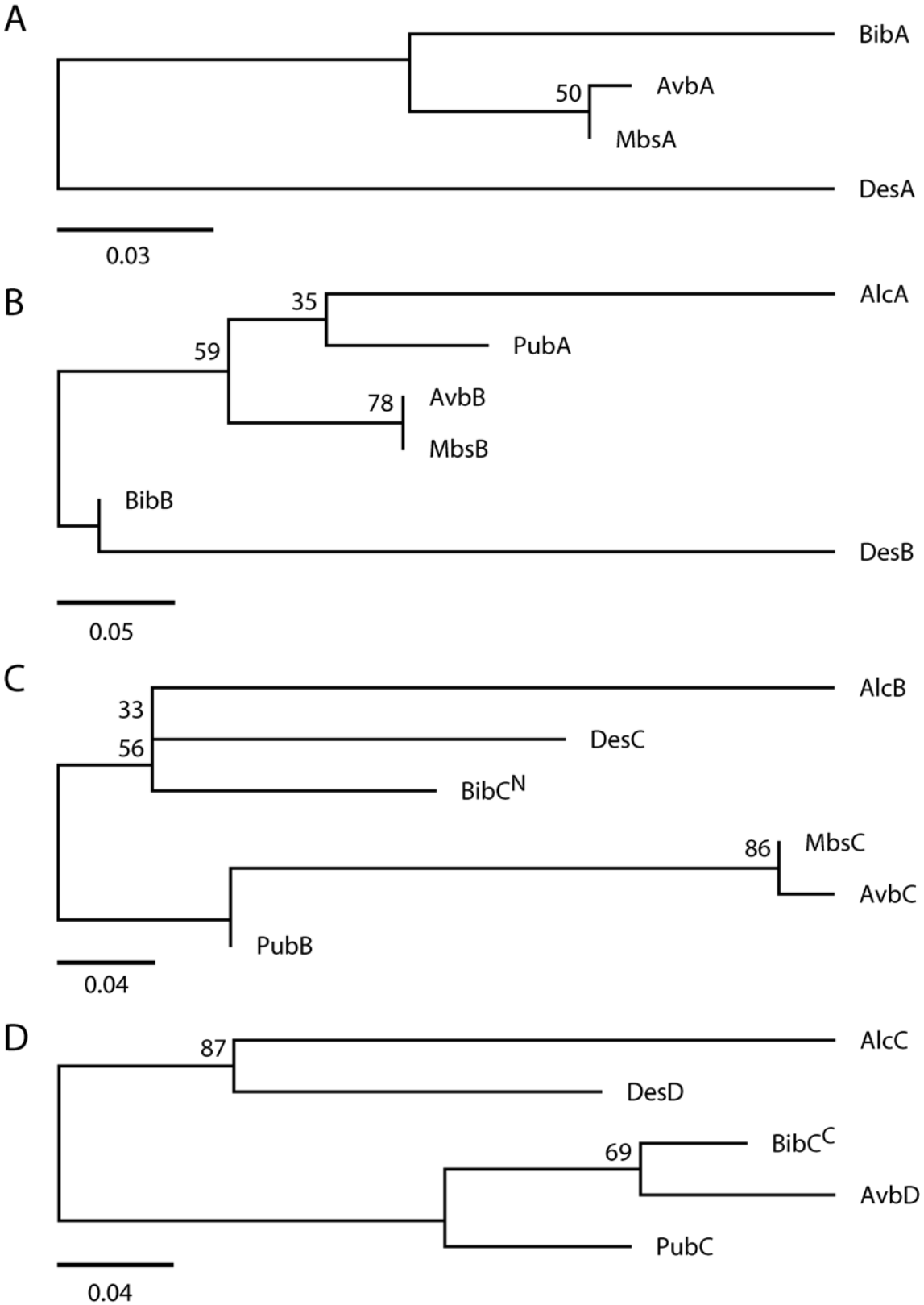

Figure S14: Maximum likelihood phylogenetic analysis of individual biosynthetic gene products of the avaroferrin gene cluster. The putative decarboxylase AvbA (A), the putative monooxygenase AvbB (B), and the two putative amide bond forming enzymes AvbC (C) and AvbD (D). Bootstrap values of 1000 re-samplings are given at branching points. The scale bars indicate 3%, 5%, 4%, and 4% amino acid substitutions per site.

Bisucaberin

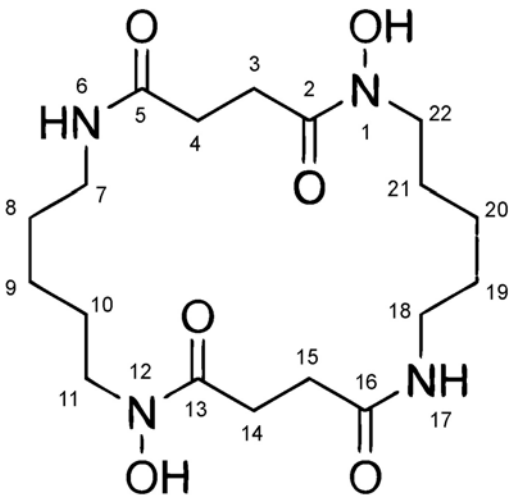

Position	DMSO-d_6	
	δ ^{1}H (multip., *J*, no. H)	δ ^{13}C*
1 /12 (N-OH)	9.87 (br s, 2H)	
2/13		172.4
3/14	2.58 (t, 7.7 Hz, 4H)	27.5
4/15	2.29 (t, 7.3 Hz, 4H)	30.4
5/16		171.5
6/17 (NH)	7.71 (br s, 2H)	
7/18	3.01 (m, 4H)	37.5
8/19	1.37 (m, 4H)	27.8
9/20	1.17 (m, 4H)	22.2
10/21	1.48 (m, 4H)	25.3
11/22	3.49 (t, 6.4 Hz, 4H)	45.8

*^{13}C δ inferred from HSQC and HMBC data

Figure S15: ^{1}H and ^{13}C NMR data for bisucaberin including chemical shifts, multiplicities, *J*-coupling and number of protons.

Putrebactin

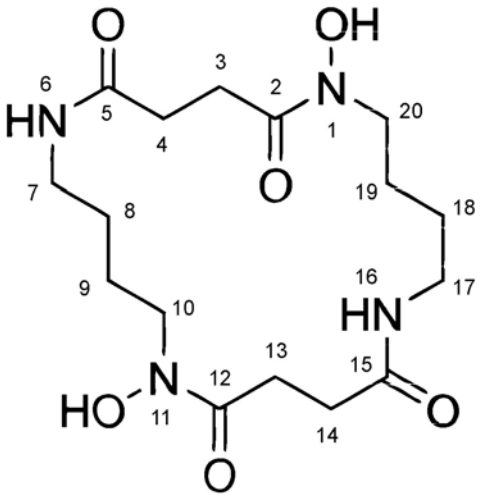

Position	DMSO-d_6	
	δ ^{1}H (multip., J, no. H)	**δ ^{13}C***
1 /11 (N-OH)	9.82 (br, 2H)	
2/12		171.5
3/13	2.59 (m, 4H)	27.4
4/14	2.28 (m, 4H)	29.7
5/15		171.3
6/16 (NH)	7.74(br s, 2H)	
7/17	3.01 (m, 4H)	37.8
8/18	1.37 (m, 4H)	25.9
9/19	1.49 (m, 4H)	23.3
10/20	3.46 (t, 7.0 Hz, 4H)	46.8

*^{13}C δ inferred from HSQC and HMBC data

Figure S16: ^{1}H and ^{13}C NMR data for putrebactin including chemical shifts, multiplicities, *J*-coupling and number of protons.

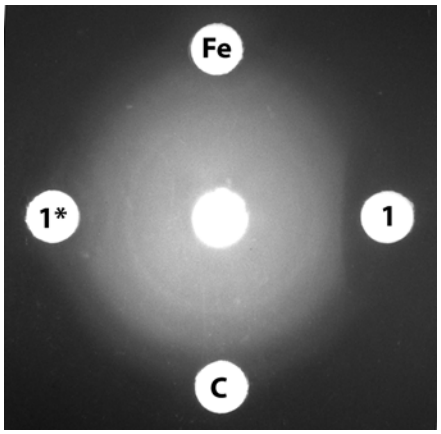

Figure S17: Effect of iron on swarming. Avaroferrin (**1**) at 50 nmol inhibited swarming of *V. alginolyticus* B522 inoculated in the center while the addition of an excess of iron chloride (10fold, **1***) neutralized the inhibition. No effect was found by 500 nmol $FeCl_3$ (**Fe**). Untreated control disc (**C**).

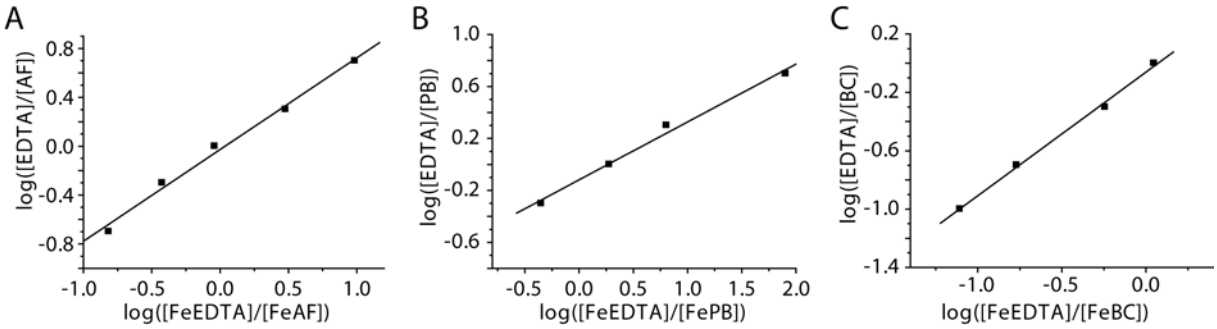

Figure S18: Spectrophotometric titration of the three siderophores with at pH 7.5 with $[Fe^{3+}]$ = [AF/PB/BC] = 0.1 mM. A) A second data set for avaroferrin resulting in a ΔpM = 0.1 ± 0.1 and a $pM(Fe^{III})$ of 23.5 ± 0.1. B) Titration of putrebactin giving a ΔpM = -0.6 ± 0.5 and a $pM(Fe^{III})$ of 22.8 ± 0.5. C) Titration of bisucaberin resulting in a ΔpM = -0.1 ± 0.1 and a $pM(Fe^{III})$ of 23.3 ± 0.1. AF: avaroferrin; PB: putrebactin; BC: bisucaberin.

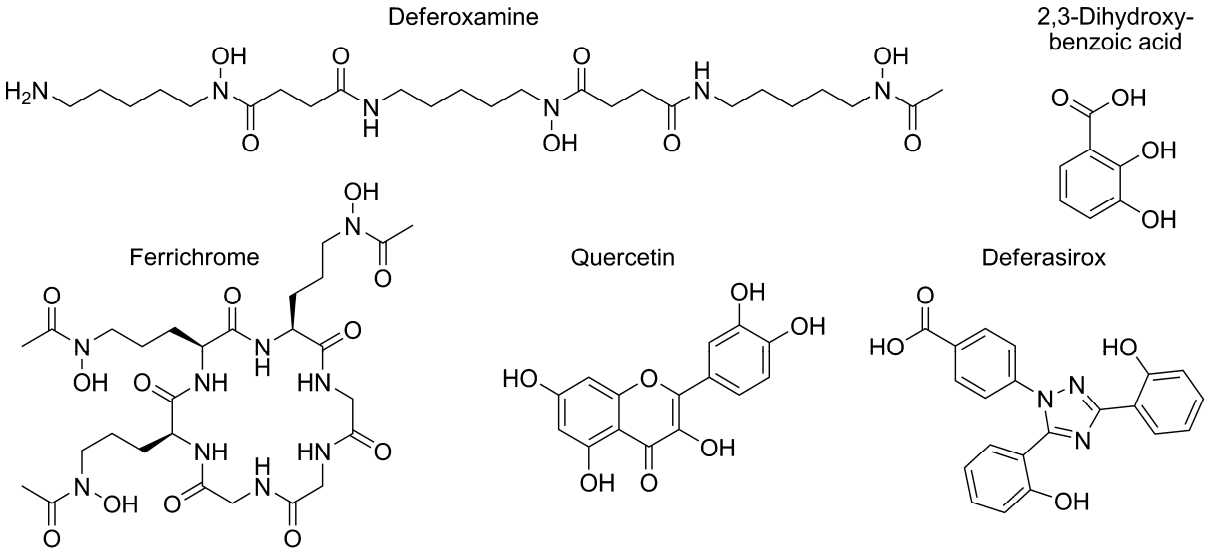

Figure S19: Structures of the different siderophores and iron chelators that were used in swarming assays.

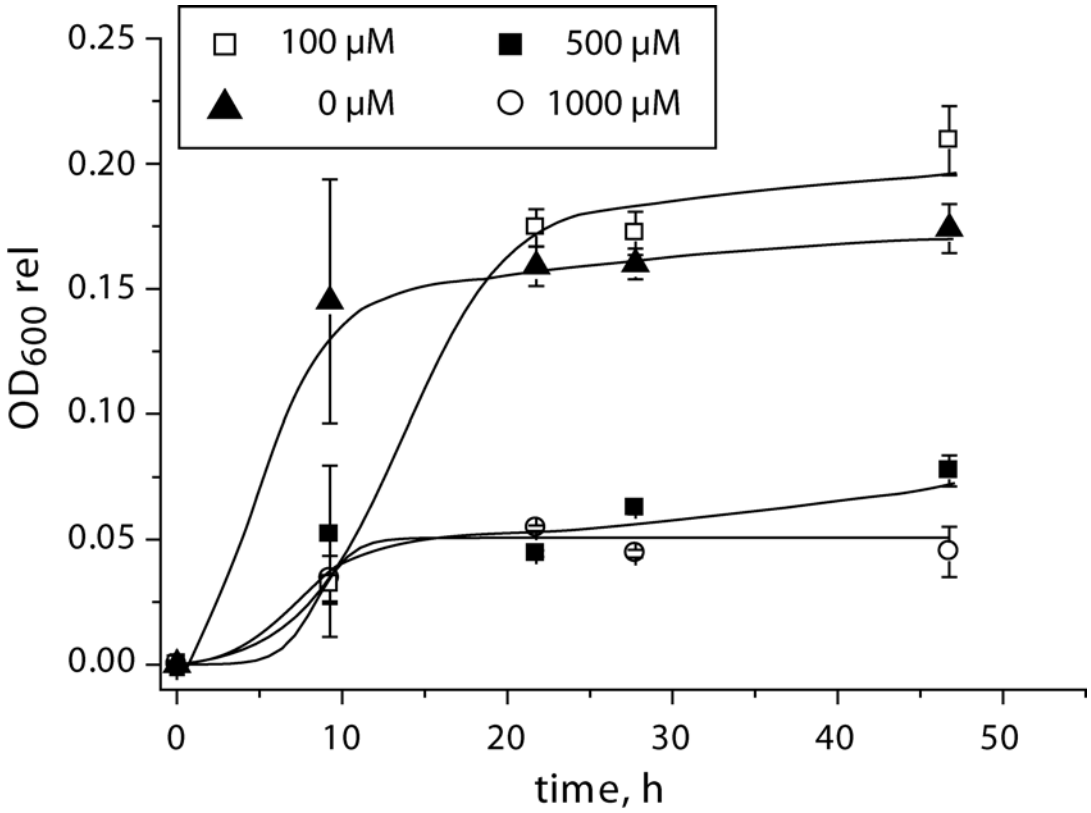

Figure S20: Growth of *V. alginolyticus* B522 in liquid culture at various concentrations of avaroferrin.

References

[1] K. Venkateswaran, D. P. Moser, M. E. Dollhopf, D. P. Lies, D. A. Saffarini, B. J. MacGregor, D. B. Ringelberg, D. C. White, M. Nishijima, H. Sano, J. Burghardt, E. Stackebrandt, K. H. Nealson, *Int J Syst Bacteriol* **1999**, *49 Pt 2*, 705.

[2] T. Böttcher, L. H. Elliott, J. Clardy, *Submitted* **2013**.

[3] G. M. Sheldrick, *Acta Crystallogr A* **2008**, *64*, 112.

[4] K. M. Ledyard, A. Butler, *J Biol Inorg Chem* **1997**, *2*, 93.

[5] A. Takahashi, H. Nakamura, T. Kameyama, S. Kurasawa, H. Naganawa, Y. Okami, T. Takeuchi, H. Umezawa, Y. Iitaka, *J Antibiot (Tokyo)* **1987**, *40*, 1671.

[6] R. J. Abergel, A. M. Zawadzka, K. N. Raymond, *J Am Chem Soc* **2008**, *130*, 2124.

[7] Z. D. Liu, R. C. Hider, *Med Res Rev* **2002**, *22*, 26.

[8] S. Dhungana, J. M. Harrington, P. Gebhardt, U. Mollmann, A. L. Crumbliss, *Inorg Chem* **2007**, *46*, 8362.